Analytical Biochemistry 464 (2014) 51–59

Contents lists available at ScienceDirect

Analytical Biochemistry

journal homepage: www.elsevier.com/locate/yabio

A nanocomposite/crude extract enzyme-based xanthine biosensor

Susan Sadeghi [a,*], Ebrahim Fooladi [a], Mohammad Malekaneh [b]

[a] Department of Chemistry, Faculty of Science, University of Birjand, Birjand, South Khorasan, Iran
[b] Department of Clinical Biochemistry, Birjand University of Medical Sciences, Birjand, South Khorasan, Iran

ARTICLE INFO

Article history:
Received 18 April 2014
Received in revised form 12 July 2014
Accepted 15 July 2014
Available online 22 July 2014

Keywords:
Biosensor
Xanthine
Crude xanthine oxidase
Fe_3O_4/polyaniline core–shell
Hybrid nanocomposite film

ABSTRACT

A novel amperometric biosensor for xanthine was developed based on covalent immobilization of crude xanthine oxidase (XOD) extracted from bovine milk onto a hybrid nanocomposite film via glutaraldehyde. Toward the preparation of the film, a stable colloids solution of core–shell Fe_3O_4/polyaniline nanoparticles (PANI/Fe_3O_4 NPs) was dispersed in solution containing chitosan (CHT) and H_2PtCl_6 and electrodeposited over the surface of a carbon paste electrode (CPE) in one step. Scanning electron microscopy (SEM), Fourier transform infrared (FTIR) spectrophotometry, cyclic voltammetry (CV), and electrochemical impedance spectroscopy (EIS) were used for characterization of the electrode surface. The developed biosensor (XOD/CHT/Pt NPs/PANI/Fe_3O_4/CPE) was employed for determination of xanthine based on amperometric detection of hydrogen peroxide (H_2O_2) reduction at −0.35 V (vs. Ag/AgCl). The biosensor exhibited a fast response time to xanthine within 8 s and a linear working concentration range from 0.2 to 36.0 μM (R^2 = 0.997) with a detection limit of 0.1 μM (signal/noise [S/N] = 3). The sensitivity of the biosensor was 13.58 μA μM^{-1} cm^{-2}. The apparent Michaelis–Menten (K_m) value for xanthine was found to be 4.7 μM. The fabricated biosensor was successfully applied for measurement of fish and chicken meat freshness, which was in agreement with the standard method at the 95% confidence level.

The quality of food products attracts much attention in human nutrition. To improve and control product quality, it is essential to know where a loss in quality is likely to occur—in the raw materials or during the process. One of the most used foods in the food diet is meat. Freshness of food is the most important criterion in a quality control approach to ensure that the product meets this criterion on a routine basis. Loss of freshness followed by spoilage is the result of a combination of complex microbiological, chemical, and physical processes [1]. Biochemical activities of microorganism contaminants in the meat lead to loss of its freshness. It is well known that after the death of animal, rapid degradation of nucleotides to hypoxanthine and then oxidation to xanthine and finally to uric acid occurs by means of the xanthine oxidase (XOD)[1] enzyme. Thus, determination of xanthine provides a useful insight into the real quality and preservation conditions of food products. Moreover, xanthine is an important biomolecule present in the human body, so that its concentration level in blood plasma and urine may provide a sensitive indicator of certain pathological states, especially for xanthinuria [2,3]. For these reasons, highly sensitive analytical methods to measure the metabolites of food degradations are needed.

Various methods for determination of xanthine have been reported, including spectrophotometry [4], high-performance liquid chromatography [5], mass spectrometry [6], capillary electrophoresis [7], fiber-optic biosensor based on a chemiluminescence reaction [8], and electrochemiluminescence biosensor [9]. Recently, some nonenzymatic and enzymatic electrochemical sensors for determination of xanthine and its metabolites have been developed [10–12]. Although these electrochemical biosensors have shown advantages such as simplicity, rapidity, high sensitivity, specificity, and low cost, they also suffer from some drawbacks such as low reproducibility, lack of stability, and slow electron transfer. To overcome some of these drawbacks, enzymes need to be immobilized onto a conductive film-coated electrode surface. Immobilization of enzymes onto the substrate surface is a critical step for the construction of enzyme-based biosensors. During recent years, various approaches have been used to immobilize enzymes onto solid substrates, including adsorption, covalent linkage, and fixer via an intermediate linker molecule [13,14]. In past few years, nanotechnology has shown remarkable potential to improve biosensors' performance in bioanalysis. Nanoparticles

* Corresponding author. Fax: +98 561 2502009.
E-mail address: ssadeghi@birjand.ac.ir (S. Sadeghi).

[1] *Abbreviations used:* XOD, xanthine oxidase; NP, nanoparticle; PANI, polyaniline; ANI, aniline; APS, ammonium peroxydisulfate; CHT, chitosan; CPE, carbon paste electrode; H_2O_2, hydrogen peroxide; HCl, hydrochloric acid; EIS, electrochemical impedance spectroscopic; FTIR, Fourier transform infrared; SEM, scanning electron microscopy; EDS, energy-dispersive X-ray spectrometer; DDW, deionized distilled water; PB, phosphate buffer; CV, cyclic voltammetry.

http://dx.doi.org/10.1016/j.ab.2014.07.013
0003-2697/

(NPs), in particular metal NPs, have shown excellent conductivity and catalytic properties that make them suitable to promote electrochemical reactions through the electron transfer between the redox centers in proteins and electrode surfaces. Among the various NPs, magnetic NPs such as Fe_3O_4 have been widely used in chemistry, medicine, and industry due to their unique magnetic and electronic properties. In electrochemical sensors, owing to advantages such as biocompatibility, large surface-to-volume ratio, high catalyst loading capacity, high dispersion, and excellent stability, magnetic NPs have been employed as alternative supports to immobilize different biomolecules and enzymes [15,16]. Moreover, incorporation of magnetic NPs into a conductive polymer matrix prevents the agglomeration of NPs. Fe_3O_4/polyaniline (Fe_3O_4/PANI) composite with regular structure has good stability, favorable solubility in organic solution, and high electrical conductivity. Two strategies can be used for electrode modification with Fe_3O_4/PANI: chemical and electrochemical polymerization. In electrochemical polymerization aniline (ANI) and Fe_3O_4 are mixed in electrochemical cells followed by electrodeposition methods, whereas in chemical polymerization a self-assembly method in the presence of HCl and ammonium peroxydisulfate (APS) has been used [17]. Most fabrication techniques for preparing nanocomposites employ chemical polymerization that mixing/compounding is more controlled than electrochemical deposition synthesis. But, for chemical deposition of the nanocomposites over the electrode surface, a cross-linker such as chitosan (CHT) is required. CHT is a natural biopolymer with biocompatibility, low toxicity, good water permeability, and high mechanical strength properties. CHT can be used extensively for enzyme immobilization through its hydroxyl and amino functional groups. Moreover, it can be deposited onto the electrode surface by applying a cathodic potential [18]. CHT can be linked to conducting polymers through covalent bonds to increase the conductivity of the formed CHT polymeric film on the electrode surface. In addition, CHT–Fe_3O_4 nanocomposite can be prepared through the simple one-step electrodeposition method [19].

Carbon paste electrodes (CPEs) have become very attractive for modifications with enzymes, particularly due to the fact that carbon pastes can be easily modified without further chemical methods. Moreover, CPEs have rather low background currents compared with solid graphite or noble metal electrodes.

In this work, a highly sensitive amperometric biosensor based on CPE modified with bovine milk crude extract of XOD coupled with CHT/Pt and PANI/Fe_3O_4 nanocomposite (XOD/CHT/Pt/PANI/Fe_3O_4/CPE) is proposed for the determination of xanthine. Integration of the PANI/Fe_3O_4 core–shell, Pt nanoparticle, and CHT components into the nanocomposite sensing material would result in synergistic electrocatalytic activity to hydrogen peroxide (H_2O_2) and improved performance of the XOD biosensor [20–22]. The proposed method is an alternative method for preparation of biosensors in which pure enzymes are used because the proposed biosensor is selective, sensitive, simple, and low cost. The enzyme electrode was employed for the determination of xanthine in tissue samples (fish and chicken), and the results were validated by the standard method.

Materials and methods

Materials

XOD (EC 1.1.3.22) was extracted from cow milk. CHT and xanthine were provided by Sigma–Aldrich (USA). $FeCl_3{\cdot}6H_2O$, $FeCl_2{\cdot}4H_2O$, APS, sodium hydroxide, hydrochloric acid (HCl), ethanol, methanol, acetone, H_2PtCl_6, and glutaraldehyde (25%) with analytical grade were purchased from Merck (Germany) and used without more purification. ANI was purified under vacuum before use.

Apparatus

All electrochemical experiments and electrochemical impedance spectroscopic (EIS) measurements were performed using a potentiostat/galvanostat equipped with an Autolab PGSTAT-302N, GPES and FRA software (EcoChemie, The Netherlands) equipped with a three-electrode system consisting of XOD/CHT/Pt/Fe_3O_4/CPE as a working electrode and Ag/AgCl and a Pt wire as reference and auxiliary electrodes, respectively. The impedance measurements were carried out over a frequency of 100 kHz to 100 mHz at an applied potential of +250 mV and using a modulation voltage of 10 mV. The Nyquist plots were modeled according to the simplified Randles circulate using Nova version 1.6 Autolab software. Fourier transform infrared (FTIR) spectra were recorded with a Vertex 70 FTIR spectrophotometer (Bruker, Germany) using KBr pellets. Scanning electron microscopy (SEM) and energy-dispersive X-ray spectrometer (EDS) analyses were performed on a LEO 1450 VP (Carl Zeiss, UK). Spectrophotometric measurements were performed on a Shimadzu 2501 PC UV–Vis (ultraviolet–visible) spectrophotometer with a 1.0-cm quartz cell (Shimadzu, Japan).

Enzyme purification and activity assay

XOD was isolated and purified from fresh bovine milk as described elsewhere [23]. The activity of the purified enzyme was measured spectrophotometrically at 295 nm based on oxidation of xanthine to uric acid according to the procedure developed by Massey and coworkers [24]. One unit of enzyme activity is defined as the amount of enzyme required to oxidize 1 mmol of xanthine per minute at 35 °C.

Preparation of Fe_3O_4/PANI core–shell

Fe_3O_4 NPs were synthesized by coprecipitation of Fe^{2+} and Fe^{3+} ions in alkaline solution under hydrothermal treatment. Subsequently, Fe_3O_4 NPs (0.25 g) were dispersed into a solution containing ANI (0.2 ml) and HCl (0.1 M), and then APS (2.2 mmol) as an oxidant was added dropwise to the solution of ANI/HCl complex [25]. The obtained nanocomposite was named Fe_3O_4/PANI.

Preparation of CHT/Pt/PANI/Fe_3O_4/CPE

First, the CPE was prepared through mixing 0.07 g of graphite powder with melted *n*-eicosane as a binder. A portion of the composite mixture was tightly packed into the end of a 1-ml propylene tube (3 mm in diameter) and was left to dry in ambient conditions. A copper wire inserted into the carbon paste provided the electrical contact. The tip of the electrode was polished with a weighing powder until the surface of the electrode had a shiny appearance, and then it was rinsed with deionized distilled water (DDW).

Second, for preparation of the modified CPE, PANI/Fe_3O_4 nanocomposite was dispersed into DDW by sonication, and then a solution containing CHT (1%, w/v) and H_2PtCl_6 (0.005 M) was added to the mixture. The mixture was stirred for 2 h at room temperature and agitated by an ultrasonic bath for 50 min. Afterward, the CHT/Pt/PANI/Fe_3O_4 nanocomposite film was formed on the cleaned surface of CPE by one-step electrodeposition of the hybrid nanocomposite at an applied potential of −1.5 V (vs. Ag/AgCl) for 60 s. The modified electrode was left to dry at room temperature. This electrode was named CHT/Pt/PANI/Fe_3O_4/CPE.

Fabrication of xanthine biosensor

For immobilization of XOD enzyme on the electrode surface, the CHT/Pt/PANI/Fe_3O_4/CPE was immersed in the solution containing

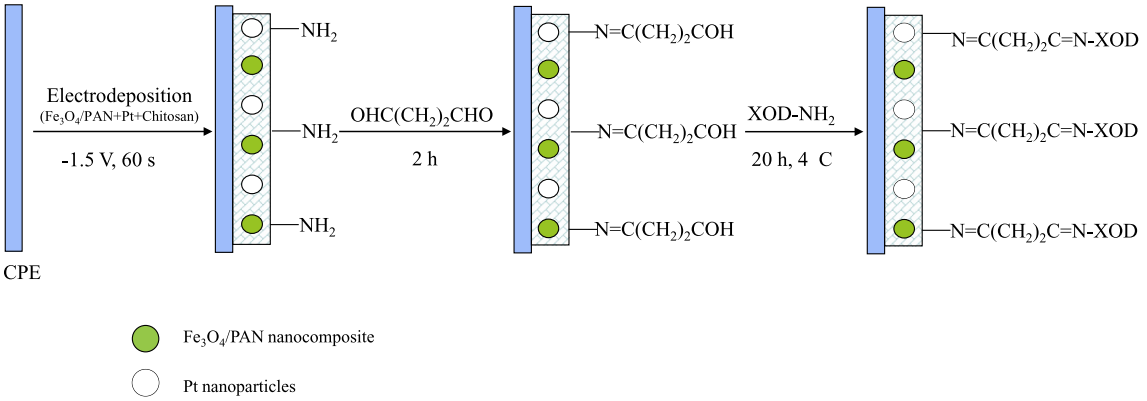

Scheme 1. Schematic representation of the preparation steps of XOD/CHT/Pt/PAN/Fe_3O_4/CPE.

glutaraldehyde (2.5%) as cross-linker for 2 h, enabling the formation of a covalent bond between the aldehyde group of glutaraldehyde and the amine group of the protein (xanthine enzyme). It provides more stable linkage than the physical aggregation. Then, the electrode was incubated in 0.2 ml of solution of the XOD with activity of 0.75 (U ml^{-1}) extracted from cow milk that was diluted 10 times with 0.05 M phosphate buffer (PB, pH 7.0, and 2 mM ethylenediaminetetraacetic acid [EDTA]) for 20 h at 4 °C. After the immobilization period, the electrode was washed five times with PB and stored at 4 °C before use. The biosensor was named XOD/CHT/Pt/PANI/Fe_3O_4/CPE. Scheme 1 summarizes reactions involved in preparation of the xanthine biosensor based on immobilization of XOD onto CHT/Pt/PANI/Fe_3O_4/CPE.

CV measurement of xanthine biosensor

Cyclic voltammetry (CV) of XOD/CHT/ Pt/PAN/Fe_3O_4/CPE was recorded in the potential range from 0.0 to −0.8 V versus Ag/AgCl as reference and using Pt wire as counter electrodes in 25 ml of 0.05 mol L^{-1} PB (pH 7.2) containing 0.2 mM xanthine. The xanthine was oxidized to uric acid and H_2O_2 as electroactive products. The performance of the proposed sensor was based on monitoring of the reduction current of H_2O_2 to H_2O on the electrode surface at −0.35 V (vs. Ag/AgCl). Hence, subsequent amperometric studies were carried out at this potential.

Determination of xanthine in fish and chicken meats

Salmon fish (3 months old) and chicken (30 days old) were prepared from a local market and were fragmented and homogenized in 5 ml of DDW and filtered through a 0.2-μm filter membrane. To obtain a clear solution with no protein, the extract was centrifuged at a speed of 11,000 rpm for 10 min. The meat samples at different storage times and conditions were prepared and determined by spectrophotometry and amperometry methods using the prepared biosensor.

Results and discussion

Characterization of PANI/Fe_3O_4 nanocomposite with FTIR

The Fe_3O_4 and PANI/Fe_3O_4 nanocomposites were characterized by FTIR spectroscopy (Fig. 1). In the spectrum of PANI/Fe_3O_4, the broad peak from 3400 to 3500 cm^{-1} was assigned to N–H stretching vibration. The absorption bands at 1592 and 1488 cm^{-1} were assigned to the quinonoid ring and benzenoid ring, respectively. The absorption bands at 1296 and 1387 cm^{-1} were related to C–N stretching absorptions and substituted –CH_3 group, respectively. The characteristic peak appearing at 571 cm^{-1} was attributed to the Fe–O stretching vibration of Fe_3O_4. The noticed shifts of absorption bands at 483 and 549 cm^{-1} confirmed the introduction of Fe_3O_4 in PANI [26]. By comparing the FTIR spectra of Fe_3O_4 (curve a) and PANI/Fe_3O_4 (curve b) in Fig. 1, it was confirmed that the magnetic NPs were successfully coated with PANI film, which was in agreement with a previous investigation [27].

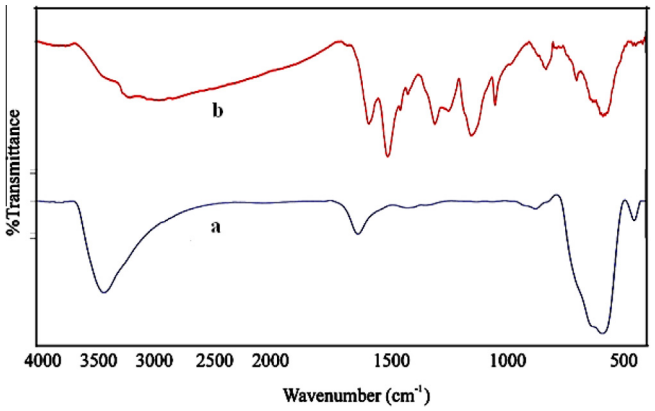

Fig.1. FTIR spectra of Fe_3O_4 (a) and PANI/Fe_3O_4 (b).

Surface characterization of working electrode by SEM

The morphology and nature of the resulting composite were characterized by SEM micrographs and EDS spectra. Fig. 2 shows representative micrographs of surface of CPE, CHT/PANI/Fe_3O_4/CPE, CHT/Pt/PANI/Fe_3O_4/CPE, and XOD/CHT/Pt/PANI/Fe_3O_4/CPE obtained by SEM. Fig. 2A shows the smooth surface of CPE, whereas the SEM image of the CHT/PANI/Fe_3O_4/CPE (Fig. 2B) illustrates that the CPE surface was mostly covered with CHT/PANI/Fe_3O_4. When Pt was electrodeposited onto CHT/PANI/Fe_3O_4, few uniform bright granular Pt NPs with minimum aggregation were observed on the modified electrode surface (Fig. 2C). The corresponding EDS spectra of Fig. 2B and C reveal the presence of Fe and Pt elements on the carbon support. Fig. 2D shows homogeneous immobilization of XOD on the surface of the modified CPE.

Surface characterization of modified electrodes by electrochemical impedance study

One of the powerful and sensitive tools that can be used in electrochemical systems for characterization of electrode surfaces is EIS. The basic approach for EIS is to apply small amplitude sine

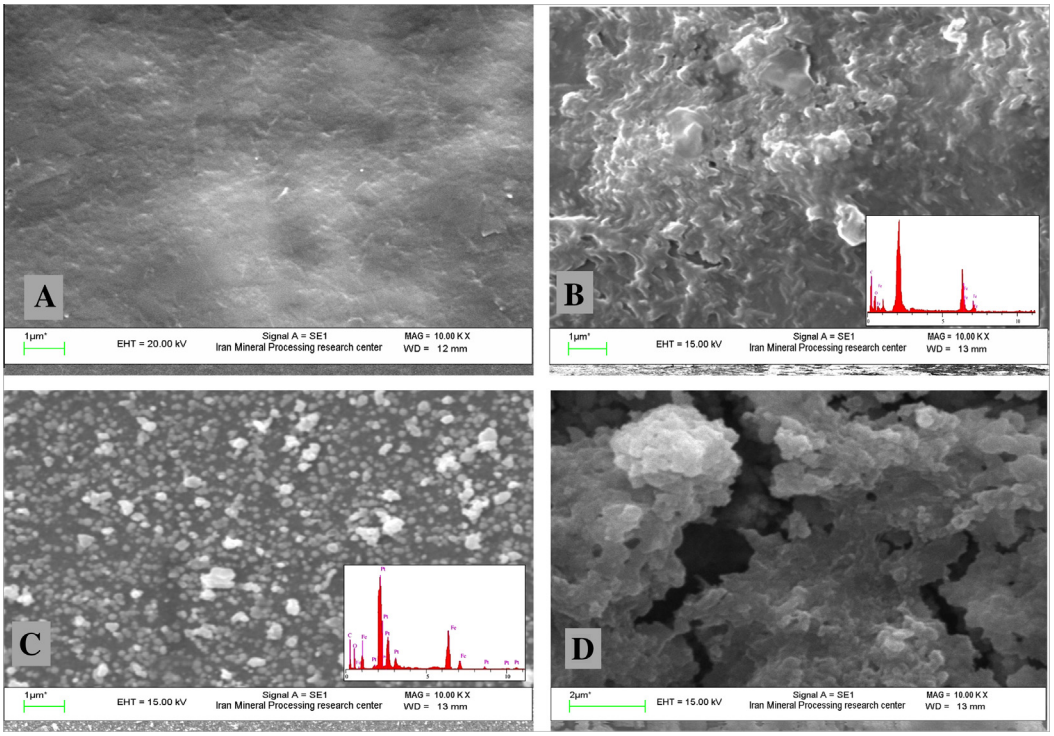

Fig.2. SEM images of CPE (A), CHT/PANI/Fe_3O_4/CPE (B), CHT/Pt/PANI/Fe_3O_4/CPE (C), and XOD/CHT/Pt/PANI/Fe_3O_4/CPE (D). Insets show the EDS spectra of CHT/PANI/Fe_3O_4/CPE and CHT/Pt/PANI/Fe_3O_4/CPE.

wave perturbations to an electrochemical system over a wide range of frequencies and measure the responding signals as a function of frequencies. The Nyquist plot is one of the most popular formats for interpretation of EIS data and consists of a semicircle followed by a straight line. The semicircle part that falls in the high-frequency range is dominated by the electron transfer process, whereas the linear portion at low frequencies corresponds to the diffusion-controlled process. The diameter of the semicircle is proportional to the electron transfer rate or electron transfer resistance (R_{ct}) of the working electrode, whereas the Warburg line indicates the mass transfer. In this work, EIS was used to characterize the stepwise modification process of the functionalized electrodes. The EIS measurements were carried out in the solution containing 0.5 mM $[Fe(CN)_6]^{3-/4-}$ redox probe in saline solution (0.1 M KCl). The equivalent circuits were used to fit the impedance spectra and extract the values of R_{ct} in each step. The corresponding Nyquist impedance plots of the modified CPEs are shown in Fig. 3A. The fitted value of R_{ct} for CHT/CPE was 680 Ω (curve a), suggesting that CHT acted as an insulating layer that made interfacial charge transfer inaccessible. The decrease in R_{ct} value of CHT/Fe_3O_4/CPE (380 Ω, curve b) revealed a reduced resistance and high electron transfer efficiency. Fig. 3A also shows that when PANI and Pt/PANI were electrodeposited on CPE (curves c and d, respectively), the diameter of the semicircle was obviously lower than that of curve a. The R_{ct} values of CHT/PANI/CPE, CHT/Pt/PANI/CPE, and CHT/Pt/PANI/Fe_3O_4/CPE were 327, 176, and 145 Ω, respectively, indicating that the nanoparticle/nanocomposite plays an important role for the improved conductivity. However, when XOD was immobilized onto CHT/Pt/PANI/Fe_3O_4/CPE surface (curve e), the diameter of the semicircle portion increased, which can be attributed to the fact that the biological molecule had low conductivity at low frequencies and hindered electron transfer. This result highlights the immobilization of XOD on CHT/Pt/PANI/Fe_3O_4/CPE as XOD/CHT/Pt/PANI/Fe_3O_4/CPE (curve f).

Surface characterization of modified electrodes by CV

Fig. 3B shows cyclic voltammograms of the above-prepared electrodes in 0.1 M KCl solution containing 5 mM $[Fe(CN)_6]^{3-/4-}$ redox probe. In this work, a hybrid nanocomposite of PANI, Fe_3O_4, and Pt nanomaterials was prepared to combine the advantages of their components. The Fe_3O_4 NPs greatly increased the effective surface area of the modified electrode, so that the peak current (I_p) gave a further increase on CHT/Fe_3O_4/CPE (curve b) than on CHT/CPE (curve a). Deposition of Pt NPs improved the electrochemical activity of the electrode. The catalytic property of Pt/PANI nanocomposite toward probe was explored by studying voltammograms of the modified CPE. Compared with CHT/PANI/CPE (curve c), the voltammogram of CHT/Pt/PANI/CPE (curve d) exhibits a decrease in ΔE_p and a prominent enhancement in I_p, clearly demonstrating that the synergistic influence of nanocomposite of Pt/PANI promotes electron transfer on the electrode surface. The voltammetric study suggests that the presence of Fe_3O_4 NPs results in increased electroactive surface area and enhanced electron transfer. Not only could the PANI/Fe_3O_4 nanocomposite prevent aggregation and oxidation Fe_3O_4 NPs, but also decoration of the magnetic NPs could provide a larger surface area of the nanocomposite. Afterward, the Pt/PANI/Fe_3O_4 was used for modification of CPE as CHT/Pt/PANI/Fe_3O_4/CPE (curve e). The decrease in analytical signals generated by XOD/CHT/Pt/PANI/Fe_3O_4/CPE (curve f) could be attributed to the efficient immobilization of XOD within the CHT polymeric layer.

Optimization of experimental parameters

XOD catalyzed the oxidation of xanthine in the presence of oxygen. The uric acid and H_2O_2 are products of oxidation of xanthine. The reduction or oxidation of H_2O_2 at the electrode can be

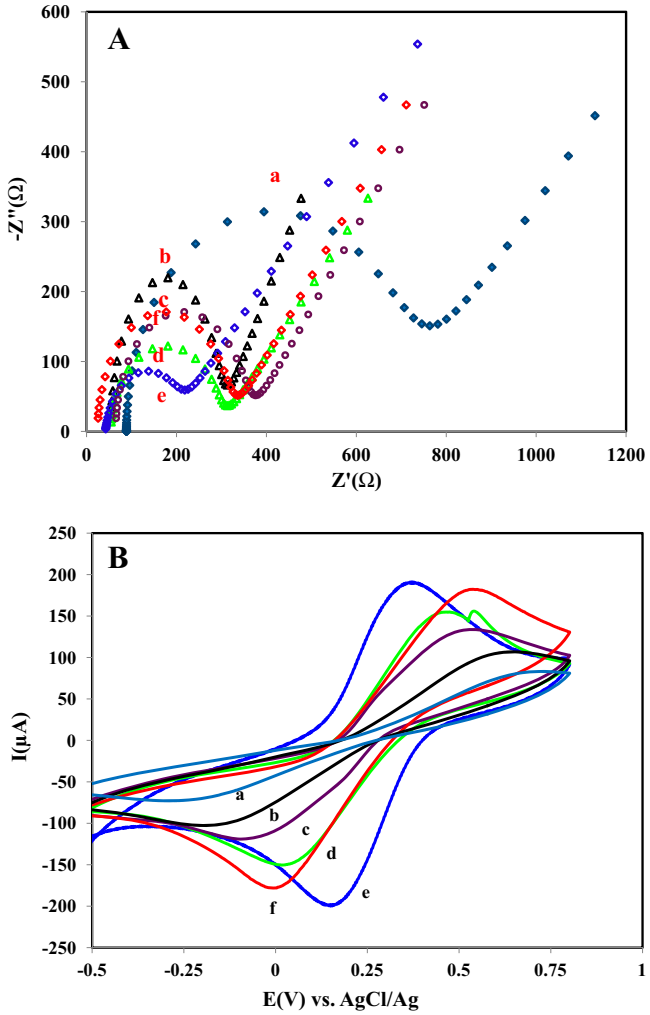

Fig.3. Electrochemical impedance spectra plots (A) and cyclic voltammograms (B) obtained with CHT/CPE (a), CHT/Fe_3O_4/CPE (b), CHT/PANI/CPE (c), CHT/Pt/PANI/CPE (d), CHT/Pt/PANI/Fe_3O_4/CPE (e), and XOD/CHT/Pt/PANI/Fe_3O_4/CPE (f) in 0.1 M KCl solution containing 5 mM $K_3Fe(CN)_6/K_4Fe(CN)_6$ (1:1) as the redox probe.

detected by amperometric XOD biosensors that can be used for indirect monitoring of xanthine concentration. However, for detection of H_2O_2 based on oxidation reactions, other electroactive materials such as uric acid and ascorbic acid interfere in the studied potential region. Thus, the reduction of H_2O_2 to H_2O was considered in this work.

The electrochemical behavior of CPE, CHT/Pt/PANI/Fe_3O_4/CPE, and XOD/CHT/Pt/PANI/Fe_3O_4/CPE was investigated by CV (Fig. 4) in a 0.05-M PB (pH 7.2) containing 200 μM xanthine in the potential range from 0.0 to −0.8 V versus Ag/AgCl at a scan rate of 50 mV/s. A significant increase in reduction peak of H_2O_2 at approximately −0.35 V (Fig. 4, curve c) was obvious for XOD/CHT/Pt/PANI/Fe_3O_4/CPE compared with CHT/Pt/PANI/Fe_3O_4/CPE (Fig. 4, curve b) and bare CPE (Fig. 4, curve a). The increase in the reduction peak current could imply that XOD immobilized on CHT/Pt/PANI/Fe_3O_4/CPE displayed good catalytic activity toward xanthine. Therefore, the working potential of −0.35 V was employed in subsequent determination of xanthine by XOD/CHT/Pt/PANI/Fe_3O_4/CPE.

The experimental conditions affecting the biosensor response were studied in terms of electrode composition and solution parameters such as Pt deposition time, XOD enzyme concentration, pH, and incubation temperature.

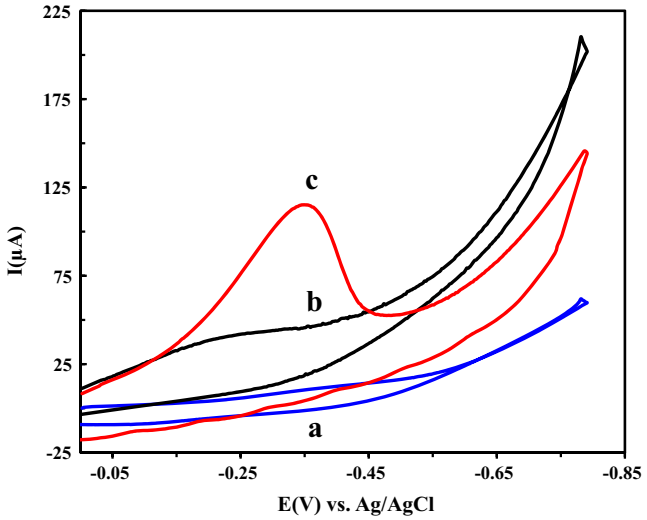

Fig.4. Cyclic voltammograms of CPE (a), CHT/Pt/PANI/Fe_3O_4/CPE (b), and XOD/CHT/Pt/PANI/Fe_3O_4/CPE (c) at 50 mV s^{-1} in PB solution (pH 7.2) containing 200 μM xanthine.

Effect of electrode composition

The Pt NPs are expected to provide a conductive path to electrons from enzyme to the electrode large surface area and catalytic activity to enhance the reduction current of H_2O_2. The electroactivity of Pt NPs for different deposition times (30–150 s) was explored by CV of the CHT/Pt/PANI/Fe_3O_4/CPE in 5 mM $[Fe(CN)_6]^{3-/4-}$ solution containing 0.1 M KCl at a scan rate of 50 mV s^{-1}. As expected, the reduction peak current increased with increasing deposition times from 30 to 60 s and decreased over 60 s. It was found that Pt particle size was enlarged and more aggregated at longer deposition times. According to the obtained results, 60 s was chosen for the electrodeposition time of Pt NPs.

The effect of enzyme concentration from 0.18 to 1.05 U ml^{-1} on the biosensor response was also studied. Fig. 5A shows that the cathodic peak current increased with increasing enzyme concentrations used up to 0.75 U ml^{-1} and then decreased. Increasing enzyme loading beyond 0.75 U ml^{-1} probably hindered electron transfer and limited enough to probe xanthine concentration. The performance of the biosensor was also firmly dependent on the enzyme loading.

Effect of temperature and pH on biosensor response

The pH and temperature display important effects on enzyme activity and biosensor performance. To obtain the optimal pH, the pH of the xanthine solution (8 μM) was varied between 5.0 and 8.5 at 37 °C. The optimal pH of the biosensor was found to be 7.2 (Fig. 5B). At pHs lower than 6.0 and higher than 8.0, the biosensor response was decreased due to the inactivation of the enzyme. The effect of temperature was investigated in the range of 20 to 45 °C. The current response increased with increasing temperatures up to 35 °C and then decreased (Fig. 5C). The lower current may be attributed to the reduced concentration of molecular oxygen in the medium and the thermal deactivation of the XOD at higher temperatures. These results showed that the response of bounded enzyme is similar to the free XOD enzyme.

Analytical performance

Fig. 6 illustrates the typical amperometric response of the biosensor based on XOD/CHT/Pt/PANI/Fe_3O_4/CPE for catalytic

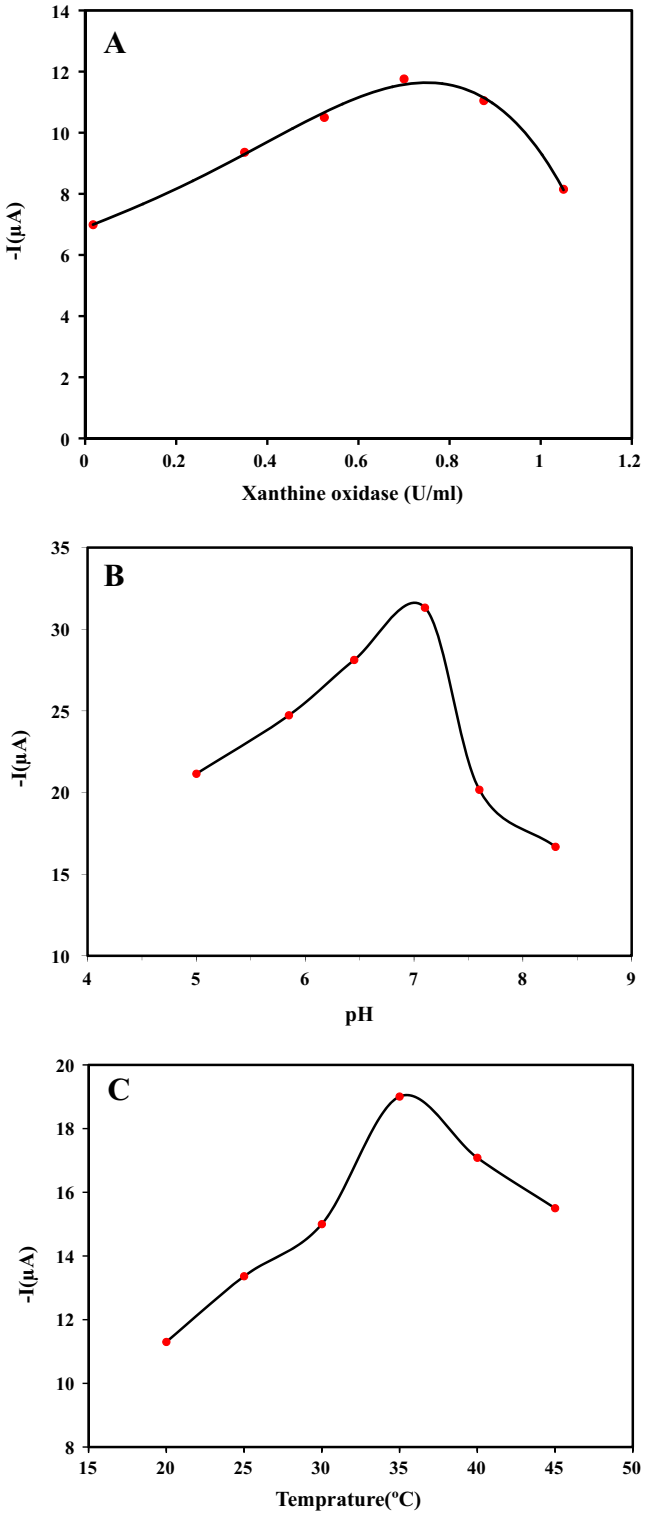

Fig.5. Effects of XOD amount (A), pH (B), and temperature (C) on amperometric response in 8 μM xanthine solution at XOD/CHT/Pt/PANI/Fe_3O_4/CPE.

oxidation of 0.2 μM xanthine in a homogeneously stirred solution containing PB (pH 7.2) at 35 °C by applying potential at −0.35 V versus Ag/AgCl. The current response increased, and the steady-state current response was achieved within 8 s for further addition of xanthine with a sample interval of 35 s. A linear relationship between current and xanthine concentration in the range of 0.2 to 36 μM (Fig. 6, inset) with a correlation coefficient of 0.997 and

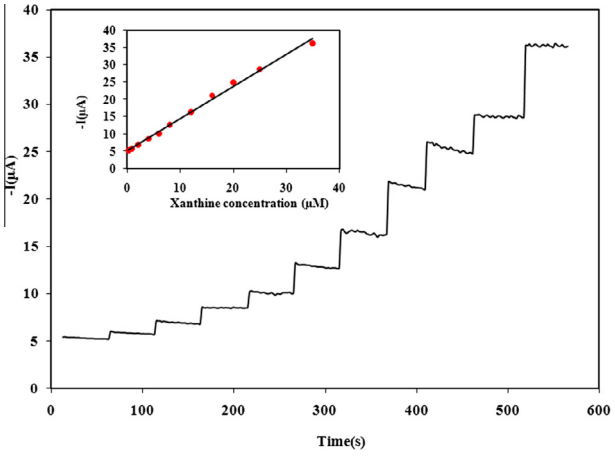

Fig.6. Chronoamperometric response of XOD/CHT/Pt/PANI/Fe_3O_4/CPE for successive addition of different xanthine concentrations in 0.05 M PB (pH 7.2). The inset shows the calibration plot drawn from current versus concentration of xanthine.

a limit of detection of 0.1 μM (signal/noise [S/N] = 3) was observed. The biosensor displayed a high sensitivity of 13.58 μA μM^{-1} cm^{-2} to xanthine. To evaluate the performance of the prepared biosensors, a comparative study of the amperometric responses of the three prepared biosensors toward xanthine, namely XOD/CHT/Pt/Fe_3O_4/CPE (Fig. 7, curve a), CHT/Pt/PANI/Fe_3O_4/CPE (Fig. 7, curve b), and XOD/CHT/CPE (Fig. 7, curve c), in a 0.05-M PB solution (pH 7.2) at a constant potential of −0.35 V was performed to quantify the sensitivity. The current response increased linearly with each xanthine addition from 0.2 to 21 μM. The current response of XOD/CHT/Pt/PANI/Fe_3O_4/CPE to xanthine was higher than that of CHT/Pt/PANI/Fe_3O_4/CPE (Fig. 7, curves a and b), indicating the role of XOD activity in oxidation of xanthine by the modified CPE. In addition, XOD/CHT/CPE (Fig. 7, curve c) showed less sensitivity to xanthine than the other two electrodes. This phenomenon was related to involvement of Pt NPs in the electrode composition that improves the biosensor performance through enhancing the direct electron transfer between the redox center of XOD and CPE.

The stability of the enzyme electrode is a very important factor that influences the application and detection performance of the biosensors. The surface stability of XOD/CHT/Pt/PANI/Fe_3O_4/CPE

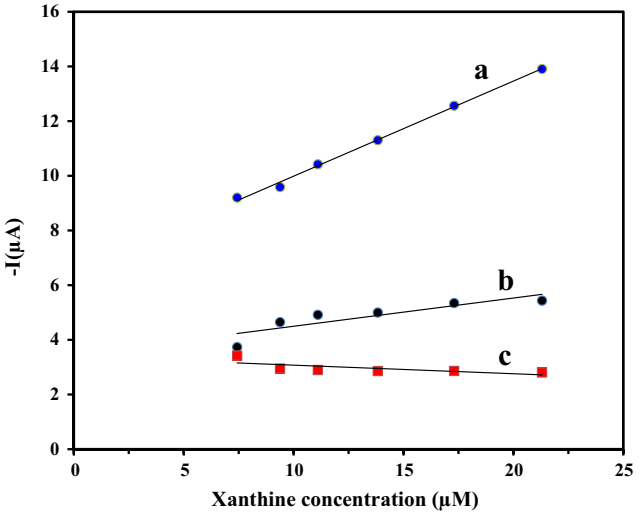

Fig.7. Comparison of the responses of XOD/CHT/Pt/PANI/Fe_3O_4/CPE (a), CHT/Pt/PANI/Fe_3O_4/CPE (b), and XOD/CHT/CPE (c) toward xanthine in 0.05 M PB (pH 7.2) at operating potential of −0.35 V (vs. Ag/AgCl).

was examined by recording several cycles voltammograms in buffer solution (pH 7.2) containing xanthine. The result showed good stability of the modified electrode with a relative standard deviation of less than 4% in cathodic peak current during five repetitive CV measurements. The long-term stability of XOD/CHT/Pt/PANI/Fe_3O_4/CPE was evaluated by measuring the amperometric response of the biosensor in 8 μM xanthine solution. The biosensor showed good long-term stability, so that the response of the biosensor still remained at 85% of its initial response after 100 uses over 3 months when stored at 4 °C.

Kinetic studies of XOD activity

Enzyme kinetics is the study of the chemical reactions that are catalyzed by enzymes. The Michaelis–Menten mechanism for the catalysis of biological chemical reactions by enzymes is one of the most important chemical reaction mechanisms in biochemistry because this mechanism can be used for measuring metabolites or inhibiting the activity of enzymes. Mostly, the Michaelis–Menten parameters such as the apparent Michaelis constant (K_m^{app}) are different for free and immobilized enzymes according to the following equation:

$$\frac{1}{I_{ss}} = \frac{1}{I_m} + \frac{K_m^{app}}{I_m \cdot S},$$

where I_{ss} is the steady-state current after the addition of substrate, I_m is the maximum current under saturated substrate conditions, and S is the substrate concentration. K_m^{app} can be obtained from the slope and the intercept of the plot of the reciprocal of the steady-state current versus the reciprocal of the substrate concentration.

The K_m^{app} value for XOD/CHT/Pt/Fe_3O_4/PAN/CPE was found to be 4.8 ± 0.4 μM, which was smaller than the K_m of free extracted enzyme (54.0 ± 2.2 μM). This low value of K_m^{app} means that the affinity of the enzyme for the substrate is high due to better accessibility of the substrate to the active sites of the immobilized enzyme.

Interference study

To evaluate the selectively of the biosensor for substrate, various metabolites such as uric acid, ascorbic acid, benzoate, and glucose as potential interferents were tested using the amperometric technique at a constant potential of −0.35 V. The amperometric responses were obtained by the addition of interfering compounds at a concentration level of 40 to 2.5 μM xanthine (Fig. 8). As can be observed from Fig. 8, the tested substances had no significant effect on the response of the xanthine biosensor. The results indicate that the performance of the biosensor at this potential was suitable for inhibition studies of XOD without interfering of the enzyme reaction products or other usual interferences.

Amperometric determination of xanthine in fish and chicken meat

The quality and safety of meats is always important for customers, particularly in the meat industry. Meat is susceptible to contamination from a wide variety of physical, biological, and chemical hazards. Because of its moisture, pH level, and high protein content, meat provides ideal environments for the growth of bacteria. Freezing of meat is a common method that can be used in meat transport. Freezing of meat increases its degradation due to cellular disruption by the freezing process. In this study, for the evaluation of the biosensor performance in real sample, the xanthine concentration in different meat samples of fish and chicken (Table 1) were determined after their storage for different time periods and under different conditions. The results show that the xanthine level increased with increasing storage times of meat samples. The experimental results were evaluated with a *t* test, and no remarkable difference between the proposed new biosensor and the standard method was observed.

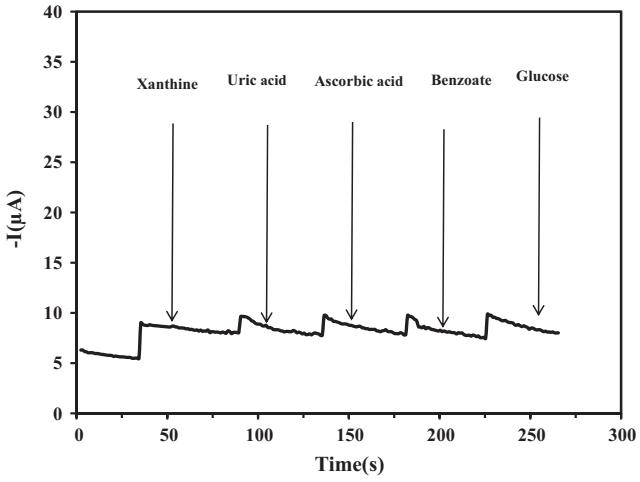

Fig.8. Amperometric response of the XOD/CHT/Pt/PANI/Fe_3O_4/CPE biosensor toward 2.5 μM xanthine on the addition of uric acid, ascorbic acid, benzoate, and glucose at a 40-μM concentration level.

Table 1
Determination of xanthine in fish and chicken sample by using the prepared biosensor.

Sample	Store conditions[a] (h)	Found by the proposed method [μmol/g (±SD)]	Found by standard method[b] [μmol/g (±SD)]	t_{exp}
Fish	6	0.56 (±0.02)	Not found	–
	24	3.73 (±0.08)	3.45 (±0.08)	0.825
	48	6.30 (±0.30)	5.40 (±0.05)	2.63
	72	8.56 (±0.15)	8.42 (±0.09)	0.495
	96	11.51 (±0.14)	10.99 (±0.14)	1.67
	120	14.89 (±0.16)	13.65 (±0.48)	2.68
	120[c]	1.47 (±0.02)	2.01 (±0.05)	3.53
Chicken	6	1.27 (±0.02)	Not found	–
	24	2.65 (±0.11)	2.45 (±0.03)	2.64
	48	3.39 (±0.20)	3.22 (±0.03)	0.620
	72	5.23 (±0.40)	5.01 (±0.06)	0.560
	96	6.34 (±0.01)	6.09 (±0.04)	1.94
	120	8.54 (±0.31)	8.36 (±0.06)	0.51
	120[c]	1.94 (±0.20)	2.57 (±0.03)	2.92

Note. SD, standard deviation; $t_{Critical}$ = 4.303; P = 0.05.
[a] Hours after death.
[b] Measured by standard method of Massey and coworkers [24].
[c] After death and stored in freezer and then 6 h stored at room temperature.

Comparison of current XOD biosensor with other reported biosensors

Table 2 compares the analytical performance of the crude extracted xanthine biosensor with that of other XOD-modified electrodes based on reduction/oxidation of enzymatically generated H_2O_2 [28–37]. The results indicate that the linear range of the new xanthine biosensor was better than that of biosensors modified with bismuth NPs and multiwalled and double-multiwalled carbon nanotubes [30,34,36]. Moreover, it has a satisfactory detection limit compared with XOD/AgNPs/L-Cys/Au, XOD/ZnO–PPy/Pt, XOD/c-MWCN/PANI/Pt, XOD/Nano-$CaCO_3$, and XOD/DWCNT/CPE [28,31–33,36] (see note at bottom of Table 2 for abbreviations). The sensitivity of the prepared biosensor for xanthine was obviously much higher than that of the other xanthine

Table 2
Comparison of current XOD biosensor with other reported biosensors.

Modified electrode	Limit of detection (μM)	Linear range (μM)	Enzyme source	Working potential (V vs. Ag/AgCl)	Sensitivity (μA μM^{-1})	References
XOD/AgNPs/l-Cys/Au	0.15	2–16	Commercial buttermilk extract	+0.50	0.20	[28]
XDH/EPG	0.00025	10–1800	Commercial *Escherichia coli* extract	+0.05	0.00031	[29]
XO/Bi NPs/CPE	0.013	0.02–0.06	Commercial buttermilk extract	−0.7	93.00	[30]
XOD/ZnO–PPy/Pt	0.8	0.8–40	Commercial buttermilk extract	+0.38	NR	[31]
XOD/c-MWCNT/PANI/Pt	0.6	0.6–58	Commercial buttermilk extract	+0.4	NR	[32]
XOD/Nano-$CaCO_3$	2.0	2–250	Commercial microbial extract	+0.55	0.021	[33]
XO/MWCNT/CPE	NR	1–100	Commercial buttermilk extract	+0.9	0.0455	[34]
XO/poly-TTCA/Pt	0.09	0.5–100	Commercial microorganism extract	−0.35	0.024	[35]
XOD/DWCNT/CPE	2	2–50	Commercial buttermilk extract	+0.9	0.0441	[36]
XOD/CoPc/CPE	NR	1000–15,000	Commercial BMT tissue extract	+0.35	NR	[37]
XOD/CHT/Pt/PANI/Fe_3O_4 NPs/CPE	0.10	0.2–36	Crude extract from buttermilk	−0.35	1.0	This work

Note. Poly-TTCA, poly-5, 2′:5′, 2″-terthiophine-3-carboxylic acid; PPy, polypyrrole; PANI, polyaniline; c-MWNT, carboxylated MWNT; CPE, carbon paste electrode; MWNT, multiwalled carbon nanotubes; NPs, nanoparticles; CNT, carbon nanotubes; CoPc, cobalt phthalocyanine; BTM, buttermilk, tissue; EPG, edge-plane pyrolytic graphite; DWCNT, double-walled carbon nanotube; PSSA-g-PPY, poly(styrenesulfonic acid-g-pyrrole); RGO, reduced graphene oxide sheet; XDH, xanthine dehydrogenase; L-Cys, L-Cysteine; NR, not reported.

biosensors [31–37]. Moreover, one of the significant advantages of the current biosensor is operation of the biosensor at low operating potential in determination of H_2O_2. This provides the possibility of application of the biosensor in determination of xanthine in real samples in the presence of other possible electroactive interferents [31–36].

Conclusion

In this work, a new application of NPs and conducting polymer for quality control of meat samples was reported. The use of Fe_3O_4/PANI and Pt NPs is attractive because of their synergistic electrocatalytic activity and signal amplification in the biosensor. According to the obtained results, it can be calculated that Fe_3O_4/PANI/Pt/CHT nanocomposite can be successfully employed for fabrication of the XOD biosensor based on crude extracted enzyme of milk. The simple procedure and using selective nanocomposites in preparation of the biosensor lead to a good reproducibility among different biosensors prepared under the same conditions. Moreover, the current method has advantages such as low cost, good stability, and reliability that should allow the developed biosensor to be used broadly in determination of xanthine in meat food products.

Acknowledgment

The authors are grateful to the Research Council of the University of Birjand for funding this work.

References

[1] H.F. Alomirah, I. Ali, B.F. Gibbs, Y. Konishi, Identification of proteolytic products as indicators of quality in ground and whole meat, J. Food Qual. 21 (1998) 299–316.
[2] J.M. Amigo, J. Coello, S. Maspoch, Three-way partial least-squares regression for the simultaneous kinetic–enzymatic determination of xanthine and hypoxanthine in human urine, Anal. Bioanal. Chem. 382 (2005) 1380–1388.
[3] V. Venugopal, Biosensors in fish production and quality control, Biosens. Bioelectron. 17 (2002) 147–157.
[4] H. Khajehsharif, E. Pourbasheer, Acid in real matrix by orthogonal signal correction–partial least squares, J. Iran. Chem. Soc. 8 (2011) 1113–1119.
[5] N. Coopera, R. Khosravanb, C. Erdmanna, J. Fienea, J.W. Lee, Quantification of uric acid, xanthine, and hypoxanthine in human serum by HPLC for pharmacodynamic studies, J. Chromatogr. B 837 (2006) 1–10.
[6] M.S. Rashed, A.A.A. Saadallah, Z. Rahbeeni, W. Eyaid, M.Z. Seidahmed, S. Al-Shahwan, M.A.M. Salih, M.E. Osman, M. Al-Amoudi, Lujane Al-Ahaidib, M. Jacob, Determination of urinary *S*-sulphocysteine, xanthine, and hypoxanthine by liquid chromatography–electrospray tandem mass spectrometry, Biomed. Chromatogr. 12 (2005) 223–230.
[7] G. Mu, F. Luan, L. Xu, F. Hu, H. Liu, Y. Gao, Determination of purines in soybean milk by capillary electrophoresis in comparison with high performance liquid chromatography, Anal. Methods 4 (2012) 3386–3391.
[8] J. Hlavay, S.D. Haemmerli, G.G. Guilbault, Fibre-optic biosensor for hypoxanthine and xanthine based on a chemiluminescence reaction, Biosens. Bioelectron. 9 (1994) 189–195.
[9] Z. Lin, J. Sun, J. Chen, L. Guo, Y. Chen, G. Chen, Electrochemiluminescent biosensor for hypoxanthine based on the electrically heated carbon paste electrode modified with xanthine oxidase, Anal. Chem. 80 (2008) 2826–2831.
[10] M.S. Ibrahim, Y.M. Temerk, M.M. Kamal, G.A.W. Ahmed, H.S.M. Ibrahim, Ultrasensitive anodic stripping voltammetry for the determination of xanthine at a glassy carbon electrode, Microchem. Acta 144 (2004) 249–256.
[11] A.C. Torres, M.E. Ghica, C.M.A. Brett, Design of a new hypoxanthine biosensor: xanthine oxidase modified carbon film and multi-walled carbon nanotube/carbon film electrodes, Anal. Bioanal. Chem. 405 (2013) 3813–3822.
[12] R. Devi, S. Yadav, C.S. Pundir, Au-colloids–polypyrrole nanocomposite film based xanthine biosensor, Colloids Surf. A 394 (2012) 38–45.
[13] R. Devi, S. Yadav, R. Nehra, S. Yada, C.S. Pundir, Sensitive and selective xanthine amperometric sensors based on calcium carbonate nanoparticles, J. Food Eng. 115 (2013) 207–214.
[14] M. Yang, Y. Yang, Y. Liu, G. Shen, R. Yu, Platinum nanoparticles–doped sol–gel/carbon nanotubes composite electrochemical sensors and biosensors, Biosens. Bioelectron. 21 (2006) 1125–1131.
[15] Y. Liu, J. Zhou, J. Gong, W.-P. Wu, N. Bao, Z.-Q. Pan, H.-Y. Gu, The investigation of electrochemical properties for Fe_3O_4@Pt nanocomposites and an enhancement sensing for nitrite, Electrochim. Acta 111 (2013) 876–887.
[16] M.S. Lin, H.J. Leu, A Fe_3O_4-based chemical sensor for cathodic determination of hydrogen peroxide, Electroanalysis 17 (2005) 2068–2073.
[17] H. Guo, H. Zhu, H. Lin, J. Zhang, Polyaniline/Fe_3O_4 nanocomposites synthesized under the direction of cationic surfactant, Mater. Lett. 62 (2008) 2196–2199.
[18] B. Krajewska, Application of chitin- and chitosan-based materials for enzyme immobilizations: a review, Enzyme Microb. Technol. 35 (2004) 126–139.
[19] S. Wanga, Y. Tana, D. Zhaoa, G. Liu, Amperometric tyrosinase biosensor based on Fe_3O_4 nanoparticles–chitosan nanocomposite, Biosens. Bioelectron. 23 (2008) 1781–1787.
[20] B.H. Nguyen, L.D. Tran, Q.P. Do, H.L. Nguye, N.H. Tran, P.X. Nguyen, Label-free detection of aflatoxin M1 with electrochemical Fe_3O_4/polyaniline-based aptasensor, Mater. Sci. Eng., C 33 (2013) 2229–2234.
[21] S. Chen, P. Fu, B. Yin, R. Yuan, Y. Chai, Y. Xiang, Immobilizing Pt nanoparticles and chitosan hybrid film on polyaniline nanofibers membrane for an amperometric hydrogen peroxide biosensor, Bioprocess Biosyst. Eng. 34 (2011) 711–719.

[22] D.A. Robinson, K.J. Stevenson, Uniform epitaxial growth of Pt on Fe_3O_4 nanoparticles: synergetic enhancement to Pt activity for the oxygen reduction reaction, J. Mater. Chem. A 1 (2013) 13443–13453.
[23] N. Ozer, M. Muftuoglu, D. Ataman, A. Ercan, I.H. Ogus, Simple, high-yield purification of xanthine oxidase from bovine milk, J. Biochem. Biophys. Methods 39 (1999) 153–159.
[24] V. Massey, G. Palmer, H. Komai, Studies on milk xanthine oxidase: some spectral and kinetic properties, J. Biol. Chem. 244 (1969) 1682–1691.
[25] A. Mehdinia, F. Roohi, A. Jabbari, Rapid magnetic solid phase extraction with in situ derivatization of methylmercury in seawater by Fe_3O_4/polyaniline nanoparticle, J. Chromatogr. A 1218 (2011) 4269–4274.
[26] S.K. El-Mahy, M. Dawy, E. Abd el Aziz, Synthesis and electrical properties of polyaniline–Fe_3O_4 nanocomposite, J. Appl. Sci. Res. 9 (2013) 2918–2926.
[27] C. Yang, J. Du, Q. Peng, R. Qiao, W. Chen, C. Xu, Z. Shuai, M. Gao, Polyaniline/Fe_3O_4 nano-particle composite: synthesis and reaction mechanism, J. Phys. Chem. B 113 (2009) 5052–5058.
[28] R. Devi, B. Batra, S. Lata, S. Yadav, C.S. Pundir, A method for determination of xanthine in meat by amperometric biosensor based on silver nanoparticles/cysteine modified Au electrode, Process Biochem. 48 (2013) 242–249.
[29] P. Kalimuthu, S. Leimkühler, P.V. Bernhardt, Low-potential amperometric enzyme biosensor for xanthine and hypoxanthine, Anal. Chem. 84 (2012) 10359–10365.
[30] U. Anik, M. Çubukçu, Application of bismuth(III)-entrapped XO biosensing system for xanthine determination in beverages, Food Anal. Methods 5 (2012) 716–722.
[31] R. Devi, M. Thakur, C.S. Pundir, Construction and application of an amperometric xanthine biosensor based on zinc oxide nanoparticles–polypyrrole composite film, Biosens. Bioelectron. 26 (2011) 3420–3426.
[32] R. Devi, S. Yadav, C.S. Pundir, Electrochemical detection of xanthine in fish meat by xanthine oxidase immobilized on carboxylated multiwalled carbon nanotubes/polyaniline composite film, Biochem. Eng. J. 58 (59) (2011) 148–153.
[33] D. Shan, Y. Wang, H. Xue, S. Cosnier, Sensitive and selective xanthine amperometric sensors based on calcium carbonate nanoparticles, Sens. Actuators B 136 (2009) 510–515.
[34] U. Anik, M. Cubukcu, Examination of the electroanalytic performance of carbon nanotube (CNT) modified carbon paste electrodes as xanthine biosensor transducers, Turk. J. Chem. 32 (2008) 711–719.
[35] M. Aminur Rahman, M.-S. Won, Y.-B. Shim, Xanthine sensors based on anodic and cathodic detection of enzymatically generated hydrogen peroxide, Electroanalysis 19 (2007) 631–637.
[36] F. Xu, I. Wang, M. Gao, L. Jin, J. Jin, Development and characterization of cobalt hexacyanoferrate modified carbon electrodes for electrochemical enzyme biosensors, Talanta 57 (2002) 365–371.
[37] E. Kilinc, A. Erdem, L. Gokgunnec, T. Dalbasti, M. Karaoglan, M. Ozsoz, Buttermilk based cobalt phthalocyanine dispersed ferricyanide mediated amperometric biosensor for the determination of xanthine, Electroanalysis 20 (1998) 273–275.